

## An all optical mapping of the strain field in GaAsN/GaAsN:H wires

M. Geddo, E. Giulotto, M. S. Grandi, M. Patrini, R. Trotta et al.

Citation: *Appl. Phys. Lett.* **101**, 191908 (2012); doi: 10.1063/1.4766285

View online: <http://dx.doi.org/10.1063/1.4766285>

View Table of Contents: <http://apl.aip.org/resource/1/APPLAB/v101/i19>

Published by the [American Institute of Physics](http://www.aip.org).

---

### Related Articles

Temperature dependent effective mass in AlGaN/GaN high electron mobility transistor structures  
*Appl. Phys. Lett.* **101**, 192102 (2012)

ZnTe/GaSb distributed Bragg reflectors grown on GaSb for mid-wave infrared optoelectronic applications  
*Appl. Phys. Lett.* **101**, 121909 (2012)

Raman spectra investigation of InAlGaN quaternary alloys grown by metalorganic chemical vapor deposition  
*J. Appl. Phys.* **112**, 063111 (2012)

Structural and micromechanical analyses by polarized Raman spectroscopy of wurtzitic GaN films grown on (0001) sapphire substrates  
*J. Appl. Phys.* **112**, 053522 (2012)

Improvement of near-infrared absorption linewidth in AlGaN/GaN superlattices by optimization of delta-doping location  
*Appl. Phys. Lett.* **101**, 102104 (2012)

---

### Additional information on *Appl. Phys. Lett.*

Journal Homepage: <http://apl.aip.org/>

Journal Information: [http://apl.aip.org/about/about\\_the\\_journal](http://apl.aip.org/about/about_the_journal)

Top downloads: [http://apl.aip.org/features/most\\_downloaded](http://apl.aip.org/features/most_downloaded)

Information for Authors: <http://apl.aip.org/authors>

## ADVERTISEMENT



**Goodfellow**  
metals • ceramics • polymers • composites  
70,000 products  
450 different materials  
small quantities fast

[www.goodfellowusa.com](http://www.goodfellowusa.com)

## An all optical mapping of the strain field in GaAsN/GaAsN:H wires

M. Geddo,<sup>1</sup> E. Giulotto,<sup>1</sup> M. S. Grandi,<sup>1</sup> M. Patrini,<sup>1</sup> R. Trotta,<sup>2,3</sup> A. Polimeni,<sup>2</sup> M. Capizzi,<sup>2</sup> F. Martelli,<sup>4</sup> and S. Rubini<sup>4</sup>

<sup>1</sup>CNISM-Dipartimento di Fisica, Università degli Studi di Pavia, Via Bassi 6, 27100 Pavia, Italy

<sup>2</sup>CNISM-Dipartimento di Fisica, Sapienza Università di Roma, Piazzale A. Moro 2, 00185 Roma, Italy

<sup>3</sup>Institute of Semiconductor and Solid State Physics, Johannes Kepler University Linz, Altenbergerstrasse 69, A-4040 Linz, Austria

<sup>4</sup>Laboratorio Nazionale TASC-IOM-CNR, Area Science Park, S.S. 14, Km. 163.5, 34012 Trieste, Italy

(Received 27 September 2012; accepted 23 October 2012; published online 9 November 2012)

GaAsN/GaAsN:H heterostructures were made by an *in-plane* selective hydrogen incorporation controlled by H-opaque metallic masks. The strain field and hydrogen distributions in GaAsN micro-sized wires thus obtained have been mapped by an all optical procedure that combines micro-Raman scattering and photoreflectance spectroscopy. The strain field is related to the formation of N-H complexes along the hydrogen diffusion profile with an ensuing expansion of the GaAsN lattice whose patterning generates an anisotropic stress in the sample growth plane. These results highlight a powerful non-invasive tool to simultaneously determine both the H diffusion profile and the related strain field distribution. © 2012 American Institute of Physics. [<http://dx.doi.org/10.1063/1.4766285>]

Recently, light polarization control in GaAsN heterostructures has been achieved by selective H-irradiation<sup>1</sup> by taking advantage from the unique property of hydrogen of forming complexes in dilute nitrides.<sup>2,3</sup> A small percentage of nitrogen incorporation produces, indeed, dramatic effects on the electronic and structural properties of the host lattice.<sup>4,5</sup> Moreover, these effects can be modified or even washed out by post-growth H-irradiation, where H passivates the electronic activity of nitrogen, thus fully restoring most of the physical properties of the N-free material.<sup>6</sup>

In GaAsN, the capability of tuning specific material parameters (e.g., band gap,<sup>7</sup> carrier effective masses,<sup>8</sup> electron g-factor,<sup>9</sup> sample resistance,<sup>10</sup> exciton binding energy,<sup>11</sup> refractive index<sup>12</sup>) via post-growth H-irradiation has been extensively investigated. The recovery of the optical and structural properties of “GaAs-like” material upon hydrogenation is accompanied by a lattice expansion along the growth direction,<sup>2,13,14</sup> which turns the tensile strain in the as-grown GaAsN layers into a compressive strain in the hydrogenated layers.<sup>15</sup> This effect accounts for an amazing, marked polarization anisotropy of the light emission observed in GaAsN/GaAsN:H wires.<sup>1</sup> This anisotropy, which develops at the *vertical* interfaces between hydrogenated and non-hydrogenated GaAsN, has been ascribed to an asymmetric distribution of the strain fields perpendicular to the wires. Beyond their interest in the basic research on semiconductors, these results have opened up the possibility to engineer the polarization properties of the light emitted by GaAsN, an alloy that can be embedded in devices based on GaAs technology.<sup>4</sup>

In this work, H distribution and related strain fields in GaAsN wires whose light polarization anisotropy has been previously investigated<sup>1</sup> are derived by an all optical procedure, which combines micro-Raman scattering and photoreflectance (PR) spectroscopy. This approach exploits the dependence on strain of the longitudinal optical (LO) phonon frequency,  $\omega^{\text{LO}}$ , and of the critical points energies at and near the energy gap as measured, respectively, by Raman scattering (on a microscopic scale) and PR (on a macroscopic

scale).<sup>16–18</sup> The combined peculiar features of the two techniques allow to get a detailed description of the strain fields and hydrogen distributions across the wires, in qualitative agreement with preliminary calculations based on the solution of a system of partial differential equations that simulate H kinetics in Ga(AsN).<sup>19</sup>

We studied a 200 nm thick GaAs<sub>0.991</sub>N<sub>0.009</sub> layer grown at 500 °C by molecular beam epitaxy on top of a GaAs buffer deposited at 600 °C on (001) GaAs substrate. N<sub>2</sub> cracking was obtained using a radio-frequency plasma source. Nitrogen concentration and layer thickness were determined by x-ray diffraction measurements. A 50 nm thick film of titanium, opaque to H, was deposited on the GaAsN surface and patterned by electron beam lithography. Samples were hydrogenated at 300 °C by a low-energy (100 eV) ion beam, then Ti masks were removed by chemical etching. The sample was hydrogenated with a H dose equal to  $3 \times 10^{18}$  ions/cm<sup>2</sup>, which allows the full depth of an unpatterned GaAsN layer to be passivated. Since H proceeds into GaAsN by a trapping-limited diffusion with a H forefront of 10 nm/decade, or less,<sup>20</sup> a steep GaAsN/GaAsN:H interface is obtained<sup>21</sup> between GaAsN wires bounded by GaAsN:H barriers that H irradiation had turned into “GaAs-like” barriers.

A sketch of the hydrogenation process used to produce the vertical interfaces defining the GaAsN wires is shown in Fig. 1. The figure displays the post-hydrogenation concentration of the electronically active N atoms (namely, N atoms not passivated by H atoms) for the case of a Ti mask of width  $w = 10 \mu\text{m}$ . Notice that the figure refers to a section of the sample near a GaAsN/GaAsN:H vertical interface. The effective N atoms distribution was calculated by extending in two dimensions and in the presence of a Ti mask, the model reported in Ref. 19.

In the investigated GaAs<sub>0.991</sub>N<sub>0.009</sub> sample, untreated wires of different widths  $w$  ( $w = 0.5, 1, 2, 5, \text{ and } 10 \mu\text{m}$ ) and directed along one of the  $\langle 110 \rangle$  directions were separated by 10–20  $\mu\text{m}$  wide hydrogenated barriers. An untreated piece of the same sample was measured for comparison’s purposes.

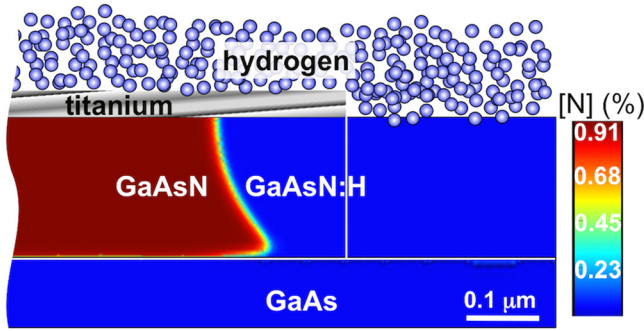


FIG. 1. Sketch of the hydrogenation process used to fabricate the GaAsN wires. View of a sample section near a GaAsN/GaAsN:H vertical interface (the actual wire is  $10\ \mu\text{m}$  wide). The wires run perpendicularly to the figure plane and the Ti wire is sketched as a greyish rectangle on the top surface. The color map shows the effective N concentration (namely, N atoms not passivated by H atoms), as derived quantitatively by extending in two dimensions and in the presence of a Ti mask the model reported in Ref. 19. The corresponding effective N concentration value is shown in a false color scale on the right.

PR measurements were performed at near-normal incidence in the 1.1–1.9 eV range, with a spectral resolution of 1 meV. A standard experimental apparatus<sup>22</sup> was operated with a 100 W halogen lamp as probe source. The excitation source was provided by a 20 mW Coherent He-Ne laser ( $\lambda = 632.8\ \text{nm}$ ; 1-mm spot diameter) chopped at 220 Hz. For Raman scattering measurements, a Jobin Yvon Labram micro-spectrometer was used. It was equipped with a  $100\times -0.90$  numerical aperture objective, a 1800 lines/mm grating, and a CCD detector. In this case, the power of the exciting He-Ne laser (spot diameter  $\sim 0.7\ \mu\text{m}$ ) was attenuated to about 1 mW to avoid light-induced dissociation of the N-H complexes.<sup>23</sup> The incident laser beam was polarized parallel to [110] axis, namely, parallel to the wires. Scans were performed in the direction  $[1\bar{1}0]$ , normal to the wires, and spectra were collected at  $0.25\ \mu\text{m}$  steps.

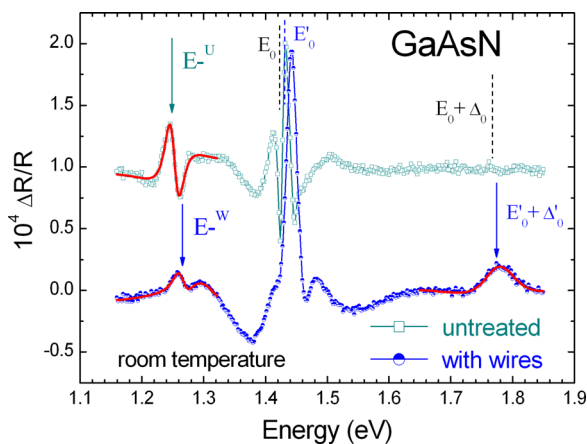


FIG. 2. Comparison of the room-temperature PR spectra of the selectively hydrogenated sample (circles) and of the untreated sample (open squares, vertically shifted for clarity). In both spectra, the PR features near 1.26 eV ( $E-w$  and  $E-u$ ) are related to the red-shifted GaAsN fundamental gap ( $E-w$  band). Note the blue-shift of the SO transition energy  $E_0' + \Delta_0'$  (due to PR signal coming from the hydrogenated sections of the sample with wires) with respect to the one of GaAs ( $E_0 + \Delta_0$ ). Arrows mark the transition energy, as obtained from the best fit (thick lines) of the experimental line-shape. The transition energy of the GaAs fundamental gap  $E_0$  and SO band  $E_0 + \Delta_0$  (literature data) as well as of the GaAsN:H fundamental gap  $E_0'$  (simulation results) is also reported (dashed bars).

In Fig. 2, the room-temperature PR spectra are shown for the selectively hydrogenated (circles) and as-grown (open squares) sample in the 1.1–1.9 eV energy range. In addition to the spectral structures (near 1.42 eV) due to the buffer/substrate GaAs band gap,<sup>18</sup> some interesting features can be clearly observed in the two spectra. In the sample with wires, the “GaAs-like” spectral features of the band gap ( $E_0'$ ) and of the split-off (SO) band ( $E_0' + \Delta_0'$ ) are due to the surface barriers between the GaAsN wires, that hydrogenation has turned into “GaAs-like” sections. These features appear greatly broadened and blue-shifted with respect to the corresponding features,  $E_0$  and  $E_0 + \Delta_0$ , reported in the literature for N-free GaAs, as previously observed.<sup>12,14</sup> These line broadening and blue-shift are due, respectively, to an increased lattice disorder and a significant *lattice expansion* in the growth plane upon H irradiation. From a best fit (thick line) of the SO spectral feature to the appropriate Aspnes line-shape model,<sup>18</sup> we estimate a value of  $(9 \pm 1)\ \text{meV}$  for the blue-shift of the SO band. With a procedure thoroughly described elsewhere,<sup>12</sup> we then derive a value of the mean compressive in-plane strain  $\varepsilon_{//}$  (in the barriers) roughly equal to  $-1.0 \times 10^{-3}$ .

The contribution to the PR spectra from the GaAsN wire sections is given by the  $E-w$  band<sup>4,5</sup> at  $E-w = 1.265\ \text{eV}$ , as determined by a best fit.<sup>24</sup> This value is 11 meV higher than that ( $E-u = 1.254\ \text{eV}$ ) derived for the same band by a best fit of the PR spectrum for the reference untreated GaAsN sample.<sup>25</sup> According to the deformation potential theory,<sup>16</sup> the energy gap increases for decreasing tensile stress (or increasing compressive strain). Therefore, on going from the untreated to the hydrogenated sample, the tensile strain *in the masked wire sections of the hydrogenated sample* should largely decrease (and eventually turn into a compressive strain), consistently with the observation of a compressive strain produced on GaAsN wires by a lattice expansion<sup>3,15</sup> in GaAsN:H barriers.<sup>1</sup>

At lower temperatures, improved experimental conditions allowed us to resolve the doublet in the  $E-w$  band of the spectra of the untreated reference sample (not shown) and to measure at  $T = 90\ \text{K}$  a valence band splitting  $\Delta E = (14 \pm 2)\ \text{meV}$ , that corresponds<sup>12,14</sup> to an in-plane tensile strain  $\varepsilon_{//} \approx +1.8 \times 10^{-3}$ , a value very close to the one expected for coherent growth of  $\text{GaAs}_{0.991}\text{N}_{0.009}$  on GaAs. Unfortunately, the same procedure failed in the case of the sample with wires. The reason may be found in the fact that the GaAsN  $E-w$  band in the hydrogenated sample is characterized by a broadening parameter somewhat greater than the one of the untreated reference sample.

The spatial distribution of the strain fields created in the patterned sample is now addressed by micro-Raman scattering measurements. Indeed, the frequency variation of the longitudinal optical mode ( $\omega^{\text{LO}}$ ) with respect to the unstrained case can nicely reproduce the actual value of the average in-plane strain, marking its enhanced compressive/tensile character for increasing/decreasing frequencies, even on a microscopic scale.<sup>26–28</sup>

In Fig. 3, we compare the room temperature Raman scattering spectra taken in different sections of the hydrogenated sample. Several lines can be identified in the spectrum taken at the center of a  $10\ \mu\text{m}$  wide GaAsN wire and are

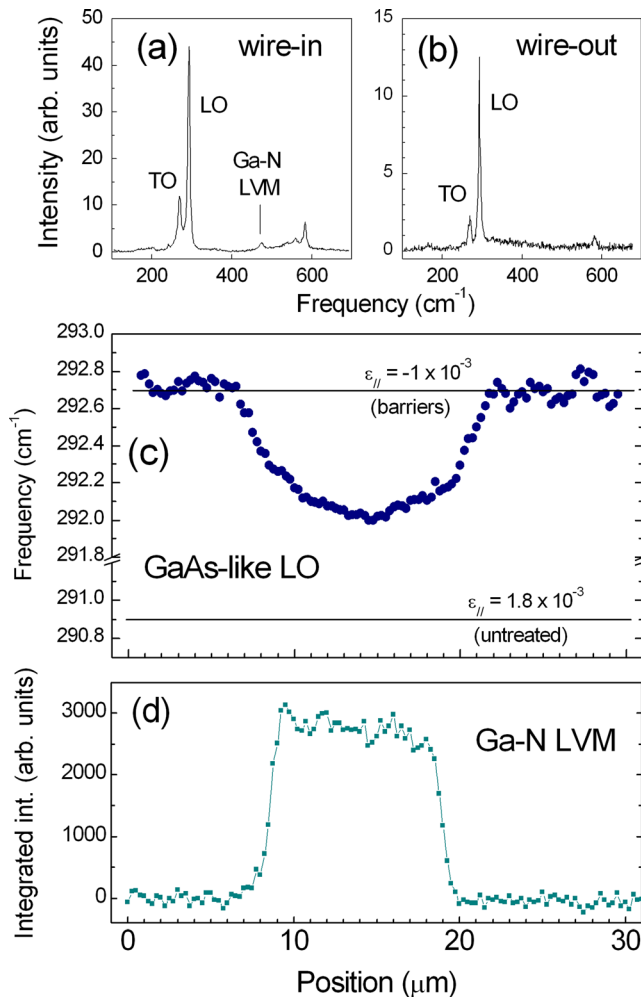


FIG. 3. (a) Room-temperature Raman spectrum taken at the center of a  $10\ \mu\text{m}$  wide GaAsN wire; (b) the same, taken in the hydrogenated barrier far from the wire axis. Note the vanishing of LVM line in the fully hydrogenated part of the barrier; (c) LO GaAs-like frequency variation along a direction perpendicular to the wire axis. The in-plane strain values derived by PR and characterizing the wire barriers and the GaAsN layer of the reference untreated sample are also reported; (d) integrated intensity of the Ga-N LVM line recorded at the same positions of panel (c).

shown in panel (a). The line at  $292.0\ \text{cm}^{-1}$  and the weaker line at  $270\ \text{cm}^{-1}$  correspond to the GaAs-like LO and TO mode, respectively (2LO and 2TO lines are also observed at double these frequencies). The line at  $475\ \text{cm}^{-1}$  is ascribed to the Ga-N local vibrational mode (LVM).<sup>13,29</sup> In panel (b), a typical spectrum taken in the hydrogenated barriers and far from the wire axis is shown. Therein, the frequency of the GaAs-like LO phonon shifts to higher values ( $292.7\ \text{cm}^{-1}$ ), in qualitative agreement with previous results.<sup>13</sup> This value is also much greater than the frequency ( $290.9\ \text{cm}^{-1}$ ) of the same Raman mode recorded in the untreated, reference sample.

In Fig. 3, panel (c), the spatial map of the frequency of GaAs-like LO line, as measured along the normal to the wire axis is displayed. The  $\omega_{\text{LO}}$  value, which is almost constant far from the wire, decreases quasi-linearly with a sudden slope change near the wire border, till it reaches a minimum at the center of the wire. On the ground of PR results, the labels in the panel indicate the different strain levels in the barrier material ( $\epsilon_{\parallel} = -1 \times 10^{-3}$ ) and in the untreated

GaAsN sample ( $\epsilon_{\parallel} = 1.8 \times 10^{-3}$ ) and the corresponding  $\omega^{\text{LO}}$  values.

In particular, our results highlight two important points. First, well into the GaAsN:H barriers the nearly constant value ( $\omega_{\text{LO}} \sim 292.7\ \text{cm}^{-1}$ ) of the GaAs-like LO frequency can be associated to the in-plane compressive strain typical of fully passivated GaAsN:H layers with similar N concentration.<sup>12,14</sup> Second, approaching the wire axial region, the net decrease of the  $\omega_{\text{LO}}$  value should correspond to an increase of the tensile character of the strain. In fact, the wire sections are subjected to the combined effect of the pre-existent biaxial tensile strain and that due to the barrier deformation induced by the H-irradiation process. Nevertheless, the observed frequency minimum is still higher than the value recorded in the untreated sample. This is likely related to the long range character that strain fields have. In turn, this leads to an effect that extends beyond the site of the H-related complexes causing the lattice expansion of GaAsN.

In Fig. 3, panel (d) shows an integrated intensity scan of the Ga-N LVM Raman line, as recorded together with data reported in panel (c). The intensity of this mode, which vanishes after hydrogenation,<sup>13</sup> is strictly related to the electrically active N concentration.<sup>30</sup> Its step-like profile confirms,<sup>20,21</sup> therefore, that a sharp hydrogen diffusion profile characterizes the vertical interfaces between hydrogenated and untreated sections of the sample.

We underline that the H diffusion profile produces a very steep interface on a  $10\ \text{nm}$  length scale.<sup>20,21</sup> Here, in the LVM intensity plot, the width of the barrier/wire interface is about  $1\ \mu\text{m}$ , clearly limited by the laser probe spot diameter. Nevertheless, by comparing the results of panels (c) and (d), one can notice that LVM intensity shows a much steeper profile, with respect to the  $\omega_{\text{LO}}$  frequency. This confirms the non local character of the strain, as mentioned before.

In summary, by combining Raman scattering and PR techniques, we produced experimental evidence of the strain field redistribution and H-diffusion profile in wire patterned GaAsN:H layers, adding useful information to those provided by micro-PL measurements. Performing an all optical mapping, the strain field behavior across the GaAsN wires was determined, highlighting its non isotropic geometry. At the same time, the presented analytical procedure allows us to monitor hydrogen diffusion profile via the quenching of the Ga-N LVM line, strictly related to the formation of N-H complexes. These results may have a relevant spin-off in engineering/realization of integrated optical circuits, where light-polarization control plays a role of primary importance in optimizing the device efficiency.

This work was partially supported by COST Action MP0805. M.G., E.G., and M.P. acknowledge Professor G. Guizzetti for fruitful discussions.

<sup>1</sup>R. Trotta, A. Polimeni, M. Capizzi, F. Martelli, S. Rubini, M. Francardi, A. Gerardino, and L. Mariucci, *Appl. Phys. Lett.* **94**, 261905 (2009).

<sup>2</sup>A. Polimeni, G. Baldassarri Höger von Högersthal, H. M. Bissirri, M. Capizzi, M. Fischer, M. Reinhardt, and A. Forchel, *Phys. Rev. B* **63**, 201304(R) (2001).

<sup>3</sup>M. Berti, G. Bisognin, D. De Salvador, E. Napolitani, S. Vangelista, A. Polimeni, M. Capizzi, F. Boscherini, G. Ciatto, S. Rubini, F. Martelli, and A. Franciosi, *Phys. Rev. B* **76**, 205323 (2007).

- <sup>4</sup>*Dilute Nitride Semiconductors*, edited by M. Henini (Elsevier, Oxford, UK, 2005).
- <sup>5</sup>*Physics, Applications of Dilute Nitrides*, edited by I. A. Buyanova and W. M. Chen (Taylor & Francis Books, Inc., New York, 2004).
- <sup>6</sup>R. Trotta, A. Polimeni, and M. Capizzi, *Adv. Funct. Mater.* **22**, 1782 (2012), and references therein.
- <sup>7</sup>M. Bissiri, G. Baldassarri Höger von Högersthal, A. Polimeni, V. Gaspari, F. Ranalli, M. Capizzi, A. Amore Bonapasta, F. Jiang, M. Stavola, D. Gollub, M. Fischer, M. Reinhardt, and A. Forchel, *Phys. Rev. B* **65**, 235210 (2002).
- <sup>8</sup>F. Masia, G. Pettinari, A. Polimeni, M. Felici, A. Miriametro, M. Capizzi, A. Lindsay, S. B. Healy, E. P. O'Reilly, A. Cristofoli, G. Bais, M. Piccin, S. Rubini, F. Martelli, A. Franciosi, P. J. Klar, K. Volz, and W. Stolz, *Phys. Rev. B* **73**, 073201 (2006).
- <sup>9</sup>G. Pettinari, F. Masia, A. Polimeni, M. Felici, A. Frova, M. Capizzi, A. Lindsay, E. P. O'Reilly, P. J. Klar, W. Stolz, G. Bais, M. Piccin, S. Rubini, F. Martelli, and A. Franciosi, *Phys. Rev. B* **74**, 245202 (2006).
- <sup>10</sup>J. Alvarez, J. P. Kleider, R. Trotta, A. Polimeni, M. Capizzi, F. Martelli, L. Mariucci, and S. Rubini, *Phys. Rev. B* **84**, 085331 (2011).
- <sup>11</sup>M. Geddo, R. Pezzuto, M. Capizzi, A. Polimeni, M. Fischer, and A. Forchel, *Eur. Phys. J. B* **30**, 39 (2002).
- <sup>12</sup>M. Geddo, T. Ciabattoni, G. Guizzetti, M. Galli, M. Patrini, A. Polimeni, R. Trotta, M. Capizzi, G. Bais, M. Piccini, S. Rubini, F. Martelli, and A. Franciosi, *Appl. Phys. Lett.* **90**, 091907 (2007).
- <sup>13</sup>P. J. Klar, H. Gruning, M. Gungerich, W. Heimbrodt, J. Koch, T. Torunski, W. Stolz, A. Polimeni, and M. Capizzi, *Phys. Rev. B* **67**, 121206(R) (2003).
- <sup>14</sup>M. Geddo, M. Patrini, G. Guizzetti, M. Galli, R. Trotta, A. Polimeni, M. Capizzi, F. Martelli, and S. Rubini, *J. Appl. Phys.* **109**, 123511 (2011).
- <sup>15</sup>G. Bisognin, D. De Salvador, A. V. Drigo, E. Napolitani, A. Sambo, M. Berti, A. Polimeni, M. Felici, M. Capizzi, M. Grungerich, P. J. Klar, G. Bais, F. Jabeen, M. Piccin, S. Rubini, F. Martelli, and A. Franciosi, *Appl. Phys. Lett.* **89**, 061904 (2006).
- <sup>16</sup>F. H. Pollak, in *Semiconductors and Semimetals*, edited by T. P. Pearsall (Academic, Boston, 1990), Vol. 32, p. 17; F. H. Pollak and M. Cardona, *Phys. Rev.* **172**, 816 (1968).
- <sup>17</sup>M. Geddo, G. Guizzetti, M. Patrini, T. Ciabattoni, L. Serravalli, P. Frigeri, and S. Franchi, *Appl. Phys. Lett.* **87**, 263120 (2005).
- <sup>18</sup>D. E. Aspnes, *Surf. Sci.* **37**, 418 (1973); D. E. Aspnes and A. A. Studna, *Phys. Rev. B* **7**, 4605 (1973); D. E. Aspnes, *Phys. Rev. B* **10**, 4228 (1974).
- <sup>19</sup>R. Trotta, D. Giubertoni, A. Polimeni, M. Bersani, M. Capizzi, F. Martelli, S. Rubini, G. Bisognin, and M. Berti, *Phys. Rev. B* **80**, 195206 (2009).
- <sup>20</sup>R. Trotta, A. Polimeni, M. Capizzi, D. Giubertoni, M. Bersani, G. Bisognin, M. Berti, S. Rubini, F. Martelli, L. Mariucci, M. Francardi, and A. Gerardino, *Appl. Phys. Lett.* **92**, 221901 (2008).
- <sup>21</sup>L. Felisari, V. Grillo, F. Martelli, R. Trotta, A. Polimeni, M. Capizzi, F. Jabeen, and L. Mariucci, *Appl. Phys. Lett.* **93**, 102116 (2008).
- <sup>22</sup>M. Geddo, G. Guizzetti, M. Capizzi, A. Polimeni, D. Gollub, and A. Forchel, *Appl. Phys. Lett.* **83**, 470 (2003).
- <sup>23</sup>N. Balakrishnan, A. Patanè, O. Makarovskiy, A. Polimeni, M. Capizzi, F. Martelli, and S. Rubini, *Appl. Phys. Lett.* **99**, 021105 (2011).
- <sup>24</sup>The strain field produces shift and splitting of GaAsN valence bands. Nevertheless, due to broadening effects, at room temperature, the doublet is unresolved in the optical response of both samples. So, a single Aspnes model function was used to derive the transition energy  $E^-$  of the GaAsN band gap.
- <sup>25</sup>In the untreated reference sample, a shoulder in the main spectral feature of the  $E^-$  band reveals, even at room temperature, its split nature.
- <sup>26</sup>H. K. Shin, D. J. Lockwood, C. Lacelle, and P. J. Poole, *J. Appl. Phys.* **88**, 6423 (2000).
- <sup>27</sup>B. Jusserand and M. Cardona, *Light Scattering in Solids V*, Topics in Applied Physics Vol. 66, edited by M. Cardona and G. Guntherodt (Springer, New York, 1989), p. 49; F. Cerdeira, C. J. Buchenauer, F. H. Pollak, and M. Cardona, *Phys. Rev. B* **5**, 580 (1972).
- <sup>28</sup>V. Bellani, C. Bocchi, T. Ciabattoni, S. Franchi, P. Frigeri, P. Galinetto, M. Geddo, F. Germini, G. Guizzetti, L. Nasi, M. Patrini, L. Seravalli, and G. Trevisi, *Eur. Phys. J. B* **56**, 217 (2007).
- <sup>29</sup>This line is absent in the spectrum collected from the hydrogenated barrier and, in agreement with previous results in Ref. 13, scattering from the GaAs-like modes is weaker in the barriers than in the GaAsN wire.
- <sup>30</sup>T. Prokofyeva, T. Sauncy, M. Seon, M. Holtz, Y. Qiu, S. Nikishin, and H. Temkin, *Appl. Phys. Lett.* **73**, 1409 (1998).